Desalination and Water Treatment
www.deswater.com

doi: 10.1080/19443994.2015.1102091

57 (2016) 19857–19864
September

Taylor & Francis
Taylor & Francis Group

Photo catalytic efficiency and kinetic studies of ZnO nanoparticles for the removal of basic dye Rhodamine B

Hiral Soni[a,*], Nirmal Kumar J.I.[a], Khushal Patel[b], Rita N. Kumar[c]

[a]*P.G. Department of Environment Science and Technology (DEST), Institute of Science and Technology for Advanced Studies and Research (ISTAR), Vallabh Vidyanagar, Gujarat 388120, India, Tel. +91 9978033036; email: hiralsoni@ymail.com (H. Soni), Tel. +91 9825968242; email: nirmalkji@gmail.com (N. Kumar J.I.)*
[b]*Department of Genetics, Ashok and Rita Patel Institute of Integrated Study and Research in Biotechnology and Allied Sciences, New Vallabh Vidyanagar, Gujarat 388121, India, Tel. +919978365630; email: khushalbiotechstudent@yahoo.co.in*
[c]*Department of Bioscience & Environment Science, N.V. Patel College of Pure and Applied Sciences, Vallabh Vidyanagar, Gujarat 388120, India, Tel. +91 9825924687; email: ritankumar@yahoo.co.in*

Received 13 April 2015; Accepted 26 September 2015

ABSTRACT

The present study reports on the photo catalytic degradation of Rhodamine B, wet chemically synthesized ZnO photocatalyst. The average particle size and shape of synthesized ZnO were 24 nm and spherical, subsequently. The experiment was carried out by irradiating the aqueous solutions of dye containing photocatalysts with UV. The rate of decolourization was estimated from residual concentration spectrophotometrically. The experiment was carried out by varying the amount of catalyst (0.5, 1, 1.5 and 2 g/L) and initial concentration of dye (10–40 mg/L). The experimental results indicated that the maximum decolourization (more than 90%) of dyes occurred with ZnO catalyst at 1.5 g/L catalyst dose. The percentage reduction of Rhodamine B was estimated under UV system. Dye adsorption equilibrium was described by the Langmuir and Freundlich adsorption isotherms over the entire concentration ranging from 10 to 40 mg/L. Adsorption data are used for modelling, from the first- and second-order kinetic equation. The characteristic results and dimensionless factors showed that ZnO nanoparticles can be employed as commercial adsorbents in the removal of Rhodamine B from aqueous solution and wastewater.

Keywords: Zinc nanoparticles; Adsorption isotherm; XRD; TEM; Rhodamine B

---

1. Introduction

Dyes are extensively used in the textile industry. They are the copious source of coloured organics emanating as a waste from the textile dyeing process. Reactive dyes have been identified as the most environmental problematic compounds in textile dye effluents [1]. Due to the high concentration of organics in the effluents and the higher stability of modern synthetic dyes, the conventional biological treatment methods are ineffective for the complete colour removal and degradation of organics and dyes [2,3]. Estimates indicate that approximately 10–20% of the synthetic textile dyes used is lost in waste streams during manufacturing or processing operations [4]. There are various methods for removal of organic and inorganic compounds from the wastewater such as

---

*Corresponding author.

filtration, electrolysis, precipitation, ion exchange and adsorption process [5,6]. The photocatalytic decomposition employing semiconductors-based photocatalysts has been a promising method for the elimination of organic pollutants in water and in the atmosphere [7–9]. Removal of dye from coloured wastewater using nanocatalyst is interesting because specific substances are transferred from liquid onto solid surface.

Many researchers have emphasized the use of TiO_2, zero-valent iron nanoparticles for the photocatalytic studies under UV radiation because of its relatively high activity and chemical stability under UV light [10,11] and they absorb only small portion of solar spectrum in UV region [12,13]. However, recently some studies have been carried out to evaluate the priority of other metal oxides [14,15]. Among the other semiconductors, ZnO appears to be a highly promising photocatalyst [16,17].

Due to high photosensitivity and large band gap, ZnO is known to be a good photocatalyst for degradation of many organic pollutants [18–20]. ZnO is one of the most important n-type semiconductor materials with a 3.37 eV band gap at room temperature and 60 meV excitation banding energy [21] that is in the UV region and makes this nanoparticle an efficient UV absorber [22,23]. It also shows remarkable potential application in catalysts [24], electrical and optical devices [25], varistors [26], gas sensors [27,28] and solar cells [29], cosmetic materials and so on. In addition, ZnO is nontoxic and environmentally friendly that is valuable for bioapplications [30].

The focus of the present work is to synthesize ZnO and use it in the photocatalytic degradation of RB (C.I. No: 45170, formula weight = 479 × 02, structure shown in Fig. 1), using UV illumination. The rate-determining parameters like initial dye concentration and catalyst loading of the dye solution on the photodegradation of RB were studied in detail. In the batch mode studies, the dynamic behaviour of the adsorption was investigated on the effect of initial metal ion concentration and adsorbent dosage. The size and shape of ZnO nanoparticles were analysed by XRD and TEM, respectively. The Langmuir, Freundlich and adsorption isotherms, adsorption kinetics were also studied.

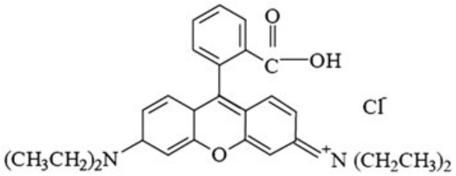

Fig. 1. Structure of Rhodamine B dye.

Double distilled water was used throughout the experiment.

2. Experimental

2.1. Synthesis of ZnO nanoparticle

ZnO nanoparticles were prepared by a wet chemical method using aqueous solution of $ZnCl_2$ (0.5 M) and NaOH (1 M) precursors as per the method of Moghaddam et al. [31] with slight modifications. From the previous study on the hydrothermal treatment of ZnO, it is clear that a raise in the NaOH concentration and experimental pH increased the ZnO particle size [32]. The focus of the present study is to obtain fine particles of ZnO as the photodegradation efficiency is proportional to the particle size of the photocatalyst used [33]. Hence, in the present study, a mild experimental pH 7 and a low concentration (1 M NaOH) solvent were considered for the synthesis experiment. Briefly, NaOH (1 M) solution was first heated to 50˚C for 5 min and then $ZnCl_2$ was added drop wise under high magnetic stirring. After addition of $ZnCl_2$, the solution was sealed and stirred for further 10 min at 50˚C till a white precipitate formed. ZnO nanoparticles containing pellet was washed three times with distilled water followed by washing with ethanol twice. Finally, ZnO nanoparticles were collected after drying the pellet at 50˚C.

2.2. Characterization of NPs

TEM analysis of NPs was characterized for their size and shape using a transmission electron microscope. Crystallographic structural analysis was carried out by an X-ray diffractometer (Shimadzu XRD-6000, Japan) [34].

2.3. Photocatalytic study

In photocatalytic experiments, 100 ml of different concentrations of RB dye (10–40 mg/L) and the catalyst dose (0.5, 1, 1.5 and 2 g/L) were taken and exposed to UV light. Dye containing tube without nanoparticles was also placed under UV to show that though during UV irradiation, direct photolysis of dyes could occur, mineralization of dyes only takes place in the presence of a photocatalyst. Dye samples of about 2–3 ml were taken out at a regular interval from the test solution, centrifuged for 4–5 min at 950–1,000 rpm and their absorbance were recorded at 555 nm using a spectrophotometer [35]. The photo degradation efficiency was calculated from the equation given below:

$$\text{Photo degradation efficiency} = \frac{\text{Initial}_{\text{OD}} - \text{Final}_{\text{OD}}}{\text{Intial}_{\text{OD}}} \times 100 \qquad (1)$$

COD was estimated before and after the treatment using $K_2Cr_2O_7$ oxidation method to measure the level of organic load in the dye solution and also to estimate the degree of degradation/mineralization of organic pollutants in the solution. The organic load is measured in terms of the total quantity of oxygen required to oxidize it into CO_2 and water. To measure COD, to 20 mL of the degraded dye solution taken in a 250-mL round bottomed flask, 0.4 g of Hg SO_4 and 10 mL of 0.25 N $K_2Cr_2O_7$ solution were added and mixed well. Then, 30 mL of H_2SO_4, $AgSO_4$ reagent (0.5 g of $AgSO_4$ in 30 mL of Conc. H_2SO_4) were added slowly with constant stirring and the mixture refluxed for 2 h. The mixture was cooled, diluted to 150 mL with distilled water and titrated against 0.25 N ferrous ammonium sulphate (FAS) solution using ferroin indicator. COD was calculated using the equation:

$$\text{COD}\ \ (\text{in mg/L}) = (V2 - V1) \times N \times 8/X \qquad (2)$$

where $V1$ and $V2$ are the volumes of FAS solution consumed by the blank and test samples, respectively, N is the normality of FAS solution and X is the volume of sample taken for analysis [36].

2.4. Adsorption studies

There are several isotherm equations available for analysing experimental sorption equilibrium parameters, the most common being the Langmuir and Freundlich models. The Langmuir isotherm model is based on the assumption that there is a finite number of active sites which are homogeneously distributed over the surface of the adsorbent These active sites have the same affinity for adsorption of a monomolecular layer and there is no interaction between the adsorbed molecules [37]. Adsorption isotherms describe the equilibrium relationship between bulk activity of adsorbate in solution and the moles adsorbed onto the surface, at constant temperature. The adsorption characteristics for a wide range of adsorbate concentration are mostly described by the adsorption isotherm (Freundlich and Langmuir), which relates the equilibrium adsorbate concentration in the bulk and the uptake of adsorbate onto the adsorbent surface. The Freundlich isotherm [38] is presented by the following relation:

$$\ln Q_e = \ln K_F + \frac{1}{n} \ln C_e \qquad (3)$$

where K_F and n are Freundlich constants, a characteristic of the system indicating the adsorption capacity and adsorption intensity, respectively.

The Langmuir isotherm [39] is valid for monolayer adsorption onto a surface containing a finite number of identical sites:

$$\frac{C_e}{Q_e} = \frac{b}{Q_0} + \frac{C_e}{Q_0} \qquad (4)$$

where C_e is the equilibrium dye concentration in the solution (mg/L), Q_e is the equilibrium dye concentration on the adsorbent (mg/g), Q_0 is the maximum adsorption capacity of the dye (forming a monolayer) per unit weight of adsorbent (mg/g) and b is a constant related to the affinity of the binding sites (L/mg).

The essential characteristics of the Langmuir isotherm can be expressed by a separation factor R_L [40], which is defined in the following equation:

$$R_L = \frac{1}{1 + bC_0} \qquad (5)$$

The R_L value shows the nature of the adsorption process to be unfavourable ($R_L > 1$), linear ($R_L = 1$), favourable ($0 < R_L < 1$) or irreversible ($R_L = 0$).

3. Result and discussion

3.1. Crystallinity and crystallite size

X-ray diffraction of ZnO surface composition is shown in Fig. 2. It indicated the surface species of prepared ZnO at 34.4 and 36.26 nm. From the half-maximum width of the fitted peaks, average crystallite sizes and size distributions of ZnO was estimated using the Scherrer equation which was found to be in the range of 26 nms [41–43].

TEM picture of the sample was taken to determine the morphology and size of the nanoparticles and compare them with the particle sizes obtained using XRD. The TEM micrograph of the ZnO nanoparticles is shown in Fig. 3 that shows hexagonal structure of ZnO nanoparticles. Similar phenomenon was observed by other researchers [44,45]. TEM results showed good agreement with the particle sizes of XRD results.

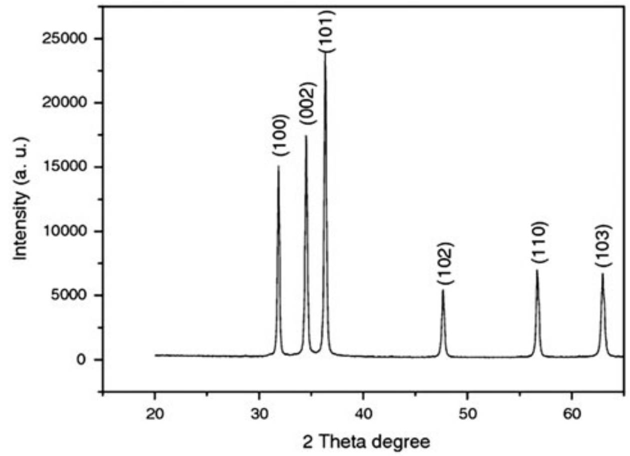

Fig. 2. XRD spectra of ZnO.

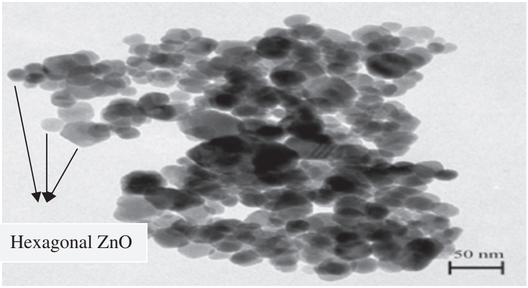

Fig. 3. TEM image of ZnO.

3.2. Photocatalytic study

The dye removal using ZnO nanoparticles without surface modification (dye: 10–40 mg/L, nanocatalyst dose: 0.5,1, 1.5, 2 g/L and pH 7) is shown in Fig. 4. The decolouration efficiency of ZnO was obtained 84, 97, 97, 90% for 0.5, 1, 1.5, 2 g/L dose for lower concentrated dye whereas higher concentrated dye gave 16, 92, 95, 55% for 0.5, 1, 1.5, 2 g/L dose, respectively. The increase in dye adsorption with adsorbent dosage is due to the increase in adsorbent surface and availability of more adsorption sites. However, at a very high dose the capacity decreased with the increasing amount of adsorbent. It can be attributed to overlapping or aggregation of adsorption sites resulting in a decrease in total adsorbent surface area available to the dye and an increase in diffusion path length. With a higher catalyst loading the deactivation of activated molecules by collision with ground state molecules dominates the reaction, thus reducing the rate of reaction [46].

The results showed that ZnO has a higher dye removal efficiency. Dye removal of 10, 20, 30 and 40 mg/L dye concentration was 90–95% for catalyst.

Table 1 gives the percentages of reduction in COD of 10, 20, 30, 40 mg/L solutions of dyes on photocatalytic treatment over ZnO for six hours. The reduction in COD values of the treated dye solutions indicates that the mineralization of dyes takes place at a slower rate when compared to the degradation of the dyes.

The amount of the dye adsorbed onto catalyst increases with an increase in the initial dye concentration of solution if the amount of the adsorbent is kept unchanged. It can be attributed to the increase in the driving force of the concentration gradient with the higher initial dye concentration. The adsorption of dye by catalyst is very intense and reaches equilibrium very quickly at a low initial concentration In other words, the residual dye concentration will be higher for higher initial dye concentrations. In the case of lower concentrations, the ratio of initial number of dye moles to the available adsorption sites is low and subsequently the fractional adsorption becomes independent of the initial concentration [47].

3.3. Equilibrium studies

As seen in Fig. 5(a), the Freundlich model described the equilibrium adsorption process. The values of the Freundlich parameters n and K_F were 1.08 and 27.48 ± 0.55 mg/g, respectively. Fig. 5(b) presents the Langmuir plot for the adsorption of Rhodamine B onto thr adsorbent. The straight line in Fig. 5(b) satisfactorily describes the Langmuir model for equilibrium adsorption process. The values of the Langmuir parameters Q_0 and b were 0.69 ± 0.55 mg/g and 0.06 L/mg, respectively. The Freundlich values indicated that the adsorption of Rhodamine B onto the adsorbent was quite fast with high adsorption capacity.

3.4. Sorption kinetics

Percentage removal of Rhodamine B at varying adsorbent doses was monitored with time. The kinetics of Rhodamine B removal by adsorbents indicated rapid binding of Rhodamine B to the sorbent during the first few minutes, followed by a slow increase until a state of equilibrium in 4 h was reached. No change in the uptake capacity was observed with further increase in equilibration time up to 8 h. The initial rapid phase may be due to increased number of vacant sites available at the initial stage, as a result

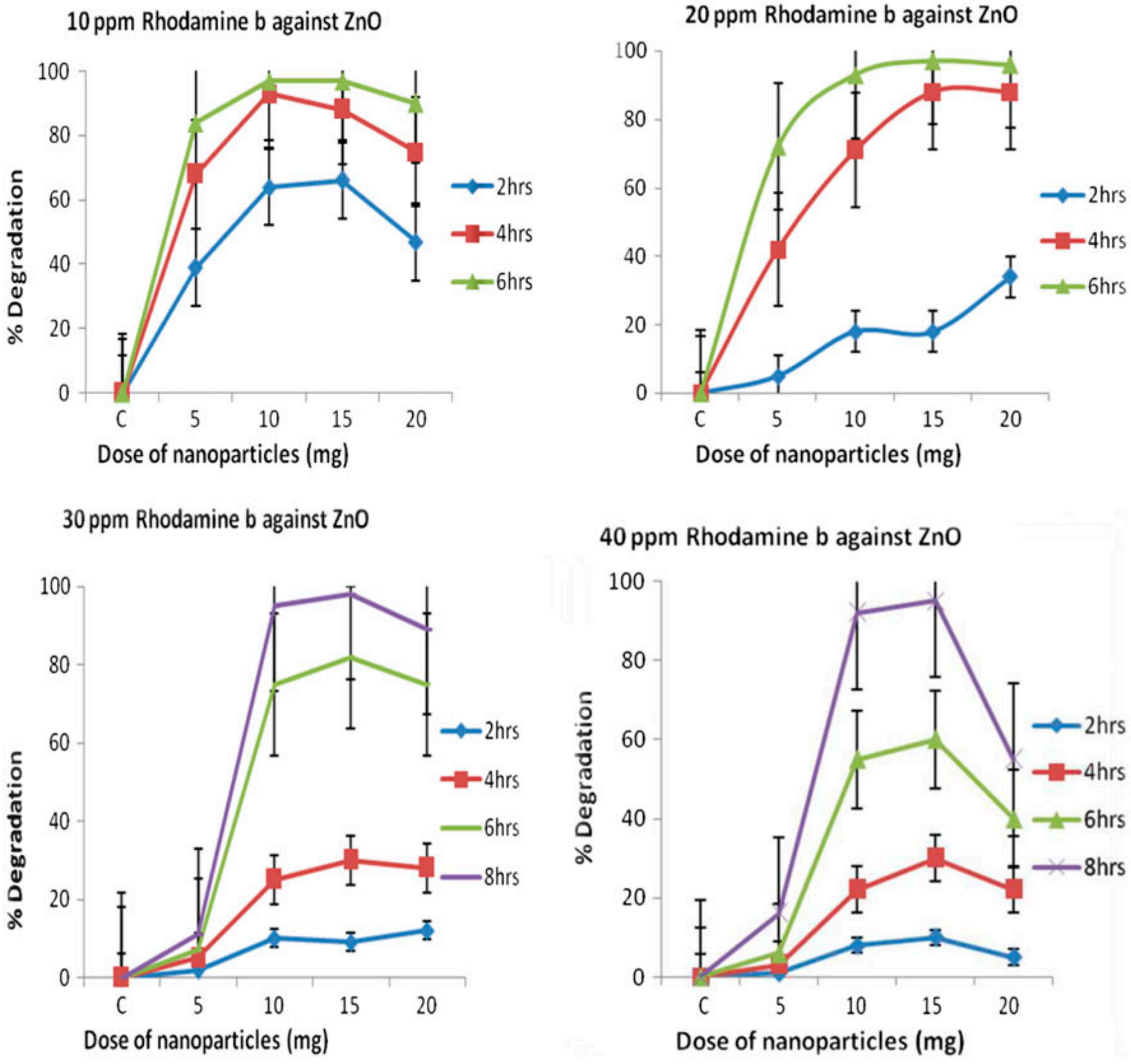

Fig. 4. Degradation of Rhodamine B by ZnO nanocatalyst.

Table 1
COD analysis of dye solution before and after treatment

Dye concentration (mg/L)	Initial sample COD	Treated sample COD	% reduction in COD
10	5.6	0.5	91
20	9.8	1.0	89
30	14.22	3.5	65
40	19.12	4.0	79

there was an increased concentration gradient between adsorbate in solution and adsorbate on the adsorbent.

Kinetics [48] of sorption was modelled by the pseudo-first and second-order equation models (Fig. 6). Lagergren's first-order rate equation is the earliest known to describe the adsorption rate based on adsorption capacity. The linear form of Lagergren's first-order rate equation is as follows [49]:

$$\ln(Q_e - Q_t) = \ln Q_e - K_1 t \qquad (6)$$

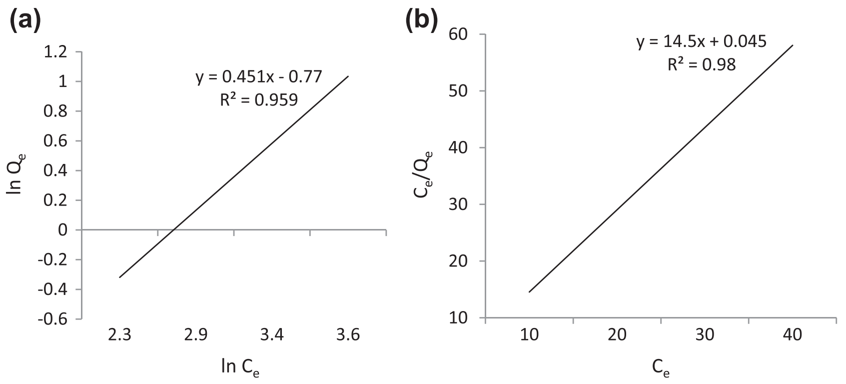

Fig. 5. (a) Freundlich isotherm plot and (b) Langmuir isotherm plot for adsorption of Rhodamine B on ZnO.

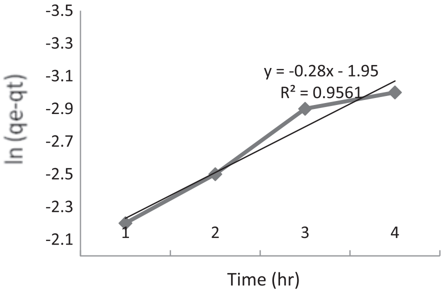

Fig. 6. Pseudo-first-order kinetic plot for the removal of Rhodamine-B onto ZnO.

The linearized form of the pseudo-second-order model as given by Ho [50] is:

$$\frac{t}{Q_t} = \frac{1}{k_2 Q_e^2} + \frac{1}{Q_e} t \tag{7}$$

where k is the pseudo-second-order rate constant of adsorption (g/mg/time unit) and Q_e and Q_t were the amount of Rhodamine B adsorbed (mg/g) at equilibrium and at time t, respectively. The adsorption kinetic data fitted best in pseudo-second-order model, where linear plot of t vs. t/Q_t was obtained.

The straight line plots of $\log(Q_e - Q_t)$ against time for the pseudo-first-order reaction, and t/Q_t against time for the pseudo-second-order reaction of the adsorption of Rhodamine-B onto ZnO are shown in Figs. 6 and 7. The correlation coefficients are closer to unity for pseudo-second-order kinetics than for pseudo-first-order kinetics. This suggests that the adsorption system can be better represented by the pseudo-second-order model.

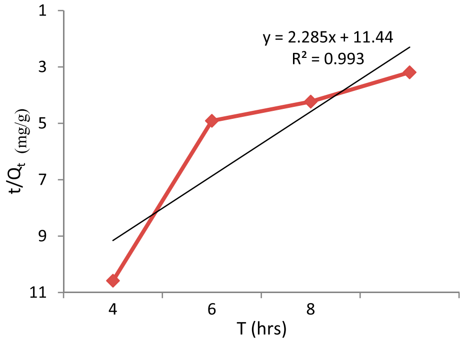

Fig. 7. Pseudo-second-order kinetic plot for the removal of Rhodamine B by ZnO.

4. Conclusion

In this paper, ZnO was synthesized and its dye removal ability was investigated. The method of synthesis was found to be significant for the formation of material with a particle size of 26 nm and hexagonal structure for ZnO. Rhodamine B was used as a model compound. 95% decoloration of dye was achieved by the catalyst. The data are well represented by the Freundlich isotherm and the Langmuir isotherm indicating favourable adsorption of Rhodamine B by the adsorbent. The data on kinetic studies indicated that the adsorption kinetics of Rhodamine B on ZnO followed the pseudo-second-order model. Study reveals that ZnO has considerable potential as an adsorbent for the removal of Rhodamine B.

References

[1] B.H. Hameed, U.G. Akpan, K.P. Wee, Photocatalytic degradation of Acid Red 1 dye using ZnO catalyst in the presence and absence of silver, Desalin. Water Treat. 27 (2011) 204–209.

[2] R.H. Souther, T.A. Alspaugh, Textile waste treatment studies, J. Water Pollut. Control Fed. 29 (1957) 918–934.

[3] A. Hamza, M.F. Hamoda, In: West Lafayette, Proc. 35th Purdue industrial waste congress, USA, 1980.

[4] N.K. Daud, U.G. Akpan, B.H. Hameed, Decolorization of sunzol black DN conc. in aqueous solution by Fenton oxidation process, effect of system parameters and kinetic study, Desalin. Water Treat. 37 (2012) 1–7.

[5] K. Lee, N.H. Lee, S.H. Shin, H.G. Lee, S.J. Kim, Hydrothermal synthesis and photocatalytic characterizations of transition metals doped nano TiO_2 sols, Mater. Sci. Eng.: B 129 (2006) 109–115.

[6] M.T. Sulak, H.C. Yatmaz, Removal of textile dyes from aqueous solutions with eco-friendly biosorbent, Desalin. Water Treat. 37 (2012) 169–177.

[7] D.F. Ollis, C.S. Turchi, Heterogeneous photocatalysis for water purification: Contaminant mineralization kinetics and elementary reactor analysis, Environ. Prog. 9 (1990) 229–234.

[8] M.R. Hoffmann, S.T. Martin, W. Choi, D.W. Bahnemann, Environmental applications of semiconductor photocatalysis, Chem. Rev. 95 (1995) 69–96.

[9] A. Mills, S.L. Hunte, An overview of semiconductor photocatalysis. J. Photochem. Photobiol., A 108 (1997) 1–35.

[10] M.C. Yeber, J. Rodríguez, J. Freer, Photocatalytic degradation of cellulose bleaching effluent by supported TiO_2 and ZnO, Chemosphere 41 (2000) 1193–1197.

[11] H. Soni, N. Kumar, K. Patel, R. Kumar, Photocatalytic decolouration of Rhodamine B dye using ZVI nanopowder synthesized by chemical reduction method, Indian J. Nanosci. 3 (2015) 1–6.

[12] J. Grzechulska, A.W. Morawski, Photocatalytic decomposition of azo-dye acid black 1 in water over modified titanium dioxide, Appl. Catal. B: Environ. 36 (2002) 45–51.

[13] M. Noorjahan, V. Durga Kumari, M. Subramanyam, Photocatalytic degradation of orange-G, Indian J. Environ. Prot. 22 (2002) 1162–1167.

[14] L.B. Reutergådh, M. Iangphasuk, Photocatalytic decolourization of reactive azo dye: A comparison between TiO_2 and us photocatalysis, Chemosphere 35 (1997) 585–596.

[15] X. Hu, L. Lei, H.P. Chu, P.L. Yue, Copper/activated carbon as catalyst for organic wastewater treatment, Carbon 37 (1999) 631–637.

[16] U. Stafford, K.A. Gray, P.V. Kamat, Photocatalytic degradation of organic contaminants: Halophenols and related model compounds, Heterogen. Chem. Rev. 3 (1996) 77–104.

[17] A.K. Carlos, G.F. Wypych, S.G. Moraes, N. Duran, N. Nagat, P.Z. Peralta, Semiconductor-assisted photocatalytic degradation of reactive dyes in aqueous solution, Chemosphere 40 (2000) 433–440.

[18] M.J. Pawar, A.D. Khajone, M.D. Gaoner, P.S. Chandel, Photodegradation Of malachite green dye over sol–gel synthesized nanocrystalline α-Fe_2O_3, Int. J. Adv. Sci. Res. Technol. 2 (2012) 471–476.

[19] N. Sobana, M. Swaminathan, Combination effect of ZnO and activated carbon for solar assisted photocatalytic degradation of Direct Blue 53, Sol. Energy Mater. Sol. Cells 91 (2007) 727–734.

[20] J. Marto, P.S. Marcos, T. Trindade, J.A. Labrincha, Photocatalytic decolouration of Orange II by ZnO active layers screen-printed on ceramic tiles, J. Hazard. Mater. 163 (2009) 36–42.

[21] Z.L. Wang, Nanostructures of zinc oxide, Mater. Today 7 (2004) 26–33.

[22] Y.Q. Li, S.Y. Fu, Y.W. Mai, Preparation and characterization of transparent ZnO/epoxy nanocomposites with high-UV shielding efficiency, Polymer 47 (2006) 2127–2132.

[23] T. Iwasaki, M. Satoh, T. Masuda, T. Fujita, Powder design for UV-attenuating agent with high transparency for visible light, J. Mater. Sci. 35 (2000) 4025–4029.

[24] Z. Dang, L. Fan, S. Zhao, C. Nan, Dielectric properties and morphologies of composites filled with whisker and nanosized zinc oxide, Mater. Res. Bull. 38 (2003) 499–507.

[25] H. Usui, Y. Shimizu, T. Sasaki, N. Koshizaki, Photoluminescence of ZnO nanoparticles prepared by laser ablation in different surfactant solutions, J. Phys. Chem. B 109 (2005) 120–124.

[26] Y. Li, G. Li, Q. Yin, Preparation of ZnO varistors by solution nano-coating technique, Mater. Sci. Eng.: B 130 (2006) 264–268.

[27] B. Baruwati, D.K. Kumar, S.V. Manorama, Hydrothermal synthesis of highly crystalline ZnO nanoparticles: A competitive sensor for LPG and EtOH, Sens. Actuators, B 119 (2006) 676–682.

[28] G.C. Yi, C. Wang, W.I. Park, ZnO nanorods: synthesis, characterization and applications, Semicond. Sci. Technol. 20 (2005) S22–S34.

[29] Z.S. Wang, C.H. Huang, Y.Y. Huang, Y.J. Hou, P.H. Xie, B.W. Zhang, H.M. Cheng, A highly efficient solar cell made from a dye-modified ZnO-covered TiO_2 nanoporous electrode, Chem. Mater. 13 (2001) 678–682.

[30] J. Zhou, N.S. Xu, Z.L. Wang, Dissolving behavior and stability of ZnO wires in biofluids: A study on biodegradability and biocompatibility of ZnO nanostructures, Adv. Mater. 18 (2006) 2432–2435.

[31] A.B. Moghaddam, T. Nazari, J. Badraghi, M. Kazemzad, Synthesis of ZnO nanoparticles and electrodeposition of polypyrrole/ZnO nanocomposite film, Int. J. Electrochem. Sci. 4 (2009) 247–257.

[32] H. Hasegawa, S. Uchida, M. Tomiha, Hydrothermal reactions, in: S.H. Feng (Ed.), Proc. Seventh International Symposium on Hydrothermal Reactions, Nishimura Tosha-do Ltd, Japan, 2003, p. 517.

[33] Z. Ding, G.Q. Lu, P.F. Greenfield, A kinetic study on photocatalytic oxidation of phenol in water by silica-dispersed titania nanoparticles, J. Colloid Interface Sci. 232 (2000) 1–9.

[34] H. Soni, N. Kumar, UV light induced photocatalytic degradation of malachite GREEN on TiO_2 nanoparticles, Int. J. Recent Res. Rev. 7 (2014) 10–15.

[35] H. Soni, N. Kumar, K. Patel, R. Kumar, Photocatalytic decoloration of three commercial dyes in aqueous phase and industrial effluents using TiO_2 Nanoparticles, Desalin. Water Treat. (Accepted), doi: 10.1080/19443994.2015.1005147.

[36] K. Byrappa, A.K. Subramani, S. Ananda, K.M. Rai, R. Dinesh, M. Yoshimura, Photocatalytic degradation of Rhodamine B dye using hydrothermally synthesized ZnO, Bull. Mater. Sci. 29 (2006) 433–438.

[37] I. Langmuir, The adsorption of gases on plane surfaces of glass, mica and platinum, J. Am. Chem. Soc. 40 (1918) 1361–1403.

[38] H. Lata, V. Garg, R. Gupta, Adsorptive removal of basic dye by chemically activated Parthenium biomass: Equilibrium and kinetic modeling, Desalination 219 (2008) 250–261.

[39] R. Liu, K. Fu, B. Zhang, D. Mei, H. Zhang, J. Liu, Removal of methyl orange by modified halloysite nanotubes, J. Dispersion Sci. Technol. 33 (2012) 711–718.

[40] I.D. Mall, V.C. Srivastava, N.K. Agarwal, I.M. Mishra, Removal of congo red from aqueous solution by bagasse fly ash and activated carbon: Kinetic study and equilibrium isotherm analyses, Chemosphere 61 (2005) 492–501.

[41] B.D. Cullity, Elements of X-Ray Diffraction, Addison-Wesley, Reading, MA, 1978.

[42] T.Y. Kim, Y. Yamazaki, Determination of the magnetic compensation composition in Al-substituted Bi-DyCoIG nanoparticles with enhanced coercive-force, IEEE Trans. Magn. 40 (2004) 2793–2795.

[43] T. Hirano, T. Namikawa, The size estimation of the Bi-YIG nanoparticles dispersed in a plastic binder, IEEE Trans. Magn. 35 (1999) 3487–3489.

[44] N. Shao-feng, L. Yong, X. Xin-hua, L. Zhang-hua, Removal of hexavalent chromium from aqueous solution by iron Nanoparticles, J. Zhejiang Univ. Sci. B 6 (2005) 1022–1027.

[45] S.R. Kanel, B. Manning, L. Charlet, H. Choi, Removal of arsenic(III) from groundwater by nanoscale zero-valent iron, Environ. Sci. Technol. 39 (2005) 1291–1298.

[46] B. Neppolian, S. Sakthivel, A. Banumathi, M. Palanichamy, V. Murugesan, ZnO-photoassisted degradation of textile dye using solar energy, Indian J. Chem. Technol. 8 (2001) 36–40.

[47] G. Crini, F. Gimbert, C. Robert, B. Martel, O. Adam, N. Morin-Crini, F. De Giorgi, P.M. Badot, The removal of Basic Blue 3 from aqueous solutions by chitosan-based adsorbent: Batch studies, J. Hazard. Mater. 153 (2008) 96–106.

[48] D.Z. Chen, J.X. Zhang, J.M. Chen, Adsorption of methyl tert-butyl ether using granular activated carbon: Equilibrium and kinetic analysis, Int. J. Environ. Sci. Technol. 7 (2010) 235–242.

[49] S. Lagergren, Kungliga Suenska Vetens kapsakademiens, Handlingar 24 (1898) 1–39.

[50] Y.S. Ho, Adsorption of Heavy Metals from Waste Streams by Peat, PhD Thesis, University of Birmingham, Birmingham, UK, 1995.